Mechanism of Ag_n Nanocluster Photoproduction from Silver Oxide Films

Lynn A. Peyser, Tae-Hee Lee, and Robert M. Dickson*

School of Chemistry and Biochemistry, Georgia Institute of Technology, Atlanta, Georgia 30332-0400

Received: May 14, 2002; In Final Form: June 25, 2002

Thin AgO films are readily photoactivated at room temperature to produce dynamic, multicolored fluorescent Ag_n nanoclusters. Writing efficiencies were separately examined as functions of excitation wavelength, intensity, and environmental interactions. The effects of external conditions on written nanocluster fluorescence are interpreted in terms of a mechanistic understanding of fluorescent Ag_n nanocluster creation and subsequent spectral dynamics, illustrating the equilibrium between nanocluster creation and destruction.

The optical and electronic properties of nanometer-sized metal particles have drawn considerable attention because of their strong, size-dependent plasmon absorptions. These strongly enhanced electromagnetic fields extremely close to the metal−medium interface enable single molecule sensitivities in surface-enhanced Raman scattering (SERS)[1] studies on Ag, Au, and Cu nanoparticles.[2−4] Control of such nanoscale optical properties has also led to applications ranging from nanosensors to waveguides.[5,6] The photoproduction of even smaller particles (2−8 atom nanoclusters) from silver halides finds important application in photography,[7,8] whereas Ag photoproduction from silver oxide has recently been utilized in near field optical storage materials.[9] Although these optical storage schemes utilize photoinduced nanoparticle formation and its near field plasmon scattering to write data, we recently discovered that significantly smaller Ag_n nanoclusters ($n = 2-8$ atoms) can also be produced from AgO films with strong, size dependent fluorescence.[10] The potential for parallel readout and increased storage capacity due to color mixing from different nanocluster distributions may further future advances in optical storage technology. Contrary to magnetic storage methods, optical storage materials are more readily expandable to 3-D architectures and can potentially store and retrieve data in parallel.

Photolytically produced from AgO, Ag nanoclusters are less than 1 nm in size, and thus not individually optically addressable. To fully utilize these photoactivated nanoclusters for high-density optical storage, we must be able to controllably write different cluster size distributions, and therefore emission colors, within each diffraction-limited spot. Such control will only be effected through detailed mechanistic understandings of Ag_n nanocluster creation dynamics. Though still limited by diffraction, the ability to write multiple properties with the same resolution increases the storage capacity by $\log_2$ (number of distinguishable states). By increasing bit depth within each data point, new optically active nanomaterials may thereby enable increased optical storage densities by encoding perceptibly different optical properties through readily controlled experimental parameters, preferably illumination intensity and time.

Thin AgO films ranging in thickness from 50 to 125 nm were produced by chemical bath deposition onto glass coverslips.[11,12] Reported to produce pure AgO, the chemical bath procedure[11,12] actually results in a mixture of oxides. Depending on the triethanolamine:$AgNO_3$ ratio, deposited film composition can range from pure silver to a mixture of AgO and Ag_2O, which we subsequently further oxidize by ozone treatment.[12] Additionally, films of pure AgO (ranging in thickness from 50 to 125 nm) were prepared by reactive RF sputtering.[13,14] The spectral dynamics of individual features were examined using green laser excitation (514.5 nm) and band-pass-filtered mercury lamp excitation. Optically interrogated in the same manner, all differently prepared AgO films exhibited similar writing ability and emission intensity, confirming AgO as the photoactive species.

Illumination of all nanocrystalline silver oxide samples with blue and UV mercury lamp excitation produces Ag_n nanoclusters that range in size from $n = 2$ to 8 atoms with strong size and geometry dependent fluorescence.[10,15−18] With the same writing wavelength, many different colored emissive species are simultaneously written to the same film. Investigating individual features on AgO films, however, becomes difficult due to the rapidly increasing fluorescence resulting from such efficient writing/photoactivation. On AgO films, each individual Ag nanocluster exhibits a unique emission pattern, indicating alignment in the $x-y$ plane.[19,20] The absence of z-oriented (perpendicular to the film) molecules and the independence of written fluorescence intensity on film thickness both indicate that the emissive Ag_n nanoclusters are surface-bound. Probing the individual features of the nanoclusters becomes much easier when they are isolated on an evaporated silver island film.[10] Because only very little AgO is present initially, the writing process does not occur rapidly, and we are able to clearly observe linearly polarized emission patterns from individual features as they slowly grow in (Figure 1). Interestingly, when unobscured by fast writing, a number of molecules oriented in the z-direction can be detected in aged, slightly oxidized Ag island films. Because oxidized silver-island films have highly curved surfaces, they are amenable to the detection of molecules oriented perpendicular to the substrate surface (Figure 1). In contrast, we have only observed $x-y$ oriented molecules on the much smoother and more homogeneous chemically deposited and RF sputtered AgO films.

To separate the photoactivation and fluorescence excitation processes in these nanomaterials, we individually wrote images (Figure 2A) with UV, blue, and green light. Each written spot was subsequently probed for fluorescence intensity with each of UV, blue, and green excitation wavelengths. (Figure 2B,C). The photoactivation efficiency clearly increases with decreasing

* Corresponding author. E-mail: dickson@chemistry.gatech.edu.

10.1021/jp026111x CCC: $22.00
Published on Web 07/24/2002

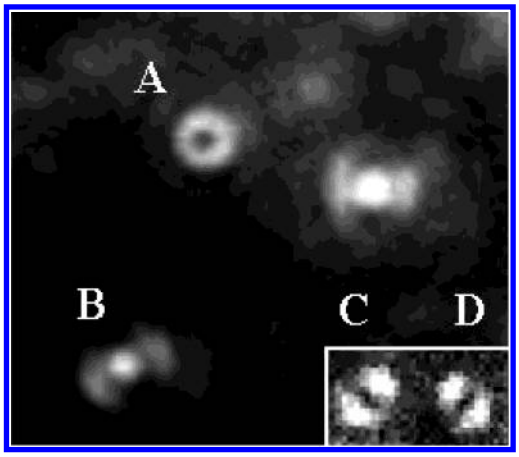

Figure 1. Typical fluorescence image from an oxidized silver-island film excited at 514.5 nm through a 1.4 numerical aperture microscope objective. Individual features appear as either doughnut (A) or bow-tie (B) patterns (when very slightly defocused); these spatial distributions of fluorescence are characteristic of individual *z*-oriented (perpendicular to the plane) and $x-y$ oriented molecules, respectively. Because of high surface curvature on oxidized Ag islands, *z*-oriented molecules are clearly observed. Although $x-y$ oriented single Ag_n nanoclusters exhibit nearly complete emission intensity modulation when passed through a rotating polarizer, these *z*-oriented molecules produce lobes parallel to the polarizer transmission axis (C, D), due to *z*-oriented molecules yielding equal amounts of *x* and *y* polarized light when collected by the microscope.

wavelength, whereas fluorescence excitation peaks in the blue. Although photoactivation of the AgO film to produce Ag_n nanoclusters is clearly much more efficient when excited with UV light, the fluorescence excitation spectrum of a written image exhibits very little UV-excited fluorescence. As these fluorescent patterns grow in through the photochemical transformation of silver oxides, this photochemical process enables small silver clusters similar to those harnessed in silver halide-based photographic emulsions to form on AgO surfaces.[7,8] Contrary to nonfluorescent Ag nanoclusters on AgBr crystals, however, nanoclusters on AgO must be better stabilized by dispersive interactions to yield fluorescence when excited with energies exceeding the gas-phase binding energy (1.68 eV for Ag_2).[21,22]

Whereas spectral diffusion has been observed in many single nanoparticle/molecule systems,[23−26] these individual emissive particles produce dynamic single particle color changes among red, orange, yellow, and green. The fluorescence dynamics within a high-density diffraction-limited spot are illustrated by dispersing the fluorescence resulting from 514 nm laser excitation with an intensity of ~3 kW/cm^2 (Figure 3). At least five distinct spectral features (548, 594, 641, 673, and 725 nm) are observed in each emission spectrum arising from distinctly differently sized and shaped Ag_n nanoclusters. These features clearly change relative intensity with time, eventually reaching a light-dependent steady-state distribution of Ag_n nanocluster sizes that produces the final spectrum/composite emission color. The same emission wavelengths are maintained throughout the experiments; only the relative intensities change with time, indicating the equilibrium among various nanocluster sizes. Indicating that multiple colors are readily written through control of sample excitation, control of final cluster size distributions should allow specific colors to be written, thereby enabling higher data storage densities to be achieved. The stabilizing and destabilizing interactions constantly increase and decrease the nanocluster size and modify molecular geometry under continuous illumination, causing the dynamic emission color changes of individual emissive sites. Thus, the time−intensity product is crucial to controlling the written cluster size distributions resulting from the equilibrium between forming and breaking apart the fluorescent Ag_n nanoclusters.

Through writing varied distributions of Ag_n clusters, different composite colors can be created with UV and blue illumination. The photoactivation (writing) process clearly only produces nanoclusters within illuminated regions of the sample, with writing rate and final fluorescent intensity strongly dependent on excitation intensity. Because each individual particle is photoactivated, data are readily stored in these AgO films. Much faster writing is easily performed at higher incident intensities from a laser source, with the rate of fluorescent nanocluster formation being strongly dependent on the incident intensity at a given wavelength. Although the final high-density image is yellow, it still exhibits bits of red and green colors, indicating that the yellow images result from color mixing of the dynamic multicolored emission observed under blue excitation. These

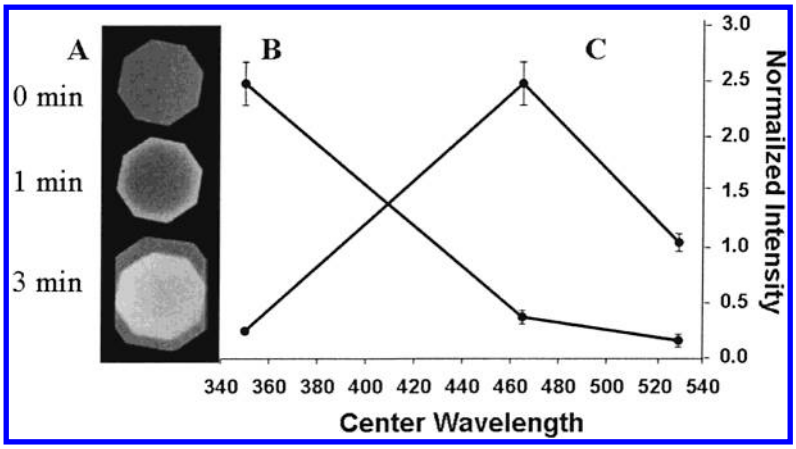

Figure 2. (A) Fluorescence written to an AgO film with mercury lamp excitation (30 W/cm^2, wavelength range: 450−480 nm). Fluorescent species are written only in the region bounded by the aperture over the 3 min illumination time. Excitation intensity is highest at the aperture edge due to diffraction; total aperture diameter is 35 microns. (B) Photoactivation spectrum of AgO films with three different Hg lamp wavelength ranges. Features similar to those in A were written with each of the three wavelength ranges (UV (340−360 nm), blue (450−480 nm), green (510−550 nm)), and probed with blue excitation, with fluorescence collected through a long pass filter. (C) Fluorescence excitation spectrum of fluorescent species written to AgO films with UV excitation. Fluorescence from written features was measured with each of UV, blue, and green excitation in ambient air conditions. All intensities within each curve are normalized to incident intensity. Error bars correspond to 90% confidence limits.

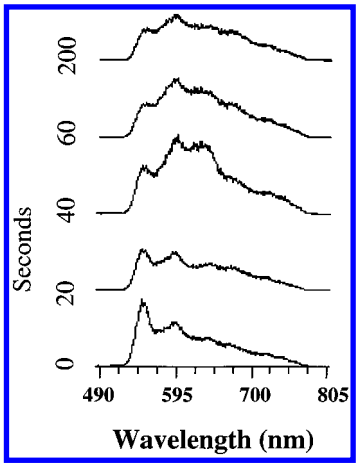

Figure 3. Typical sequential emission spectra from a ~600 nm diameter region of an AgO film excited at 514.5 nm (1 kW/cm^2) and collected through a long pass filter. At least five distinct spectral features (548, 594, 641, 673, and 725 nm) can be seen alternating in relative intensity as the Ag_n nanocluster size distribution is continuously modified through excitation. Whereas changes occur rapidly early in the spectral trajectory, the nanocluster distribution reaches a final equilibrium after ~60 s, as indicated by only minor subsequent fluctuations in relative intensity.

written images on AgO films are quite stable in the dark for several days, even when otherwise exposed to ambient conditions. Also written with UV excitation, strong red and near-IR fluorescent features are simultaneously observed within the illuminated region, which can be more efficiently excited with green excitation.

Investigations of the intensity dependent initial writing rate and final written fluorescence intensity demonstrate the light dependent equilibrium present in these systems (Figure 4). The three different curves each show an initial sharply rising linear portion, eventually reaching an equilibrium written intensity. After the final nanocluster distribution and limiting written fluorescence intensity are reached, continued reading of fluorescence causes no further observed changes. Whereas incident intensities were only varied by just over 1 order of magnitude, the final fluorescence intensities changed by 2 orders of magnitude. The initial slope (or writing rate) also exhibits a superlinear intensity dependence, indicating that multiple photons are involved in creating the fluorescent species, yielding an intensity dependence scaling as $I^{1.64\pm0.10}$. This excitation intensity dependence reflects the dynamic light-dependent equilibrium underlying the creation and destruction of multiatom Ag_n nanoclusters.

Because the incident intensity is proportional to the emission in neither a linear nor a quadratic fashion, the creation dynamics do not result from simply single-photon or two-photon processes. Because dimers and larger nanoclusters must be created to produce fluorescence, at least two independent photochemical reactions of AgO must occur ($2AgO + 2h\nu \rightarrow 2Ag + 2O^{\bullet}$), suggesting a second-order process with respect to incident intensity. Because excitation energies exceeding gas-phase nanocluster binding energies are used to excite fluorescence, a light-dependent equilibrium is established between the creation and destruction of the nanoclusters. The light dependent equilibrium between nanocluster creation and destruction is evidenced by the light-dependent blinking dynamics,[10,27] our observed relative intensity changes of emission peaks (Figure 3), and the light-dependent final fluorescence intensity for a given written feature (Figure 4). Although both forward and reverse reaction rates are light-dependent, the forward reaction

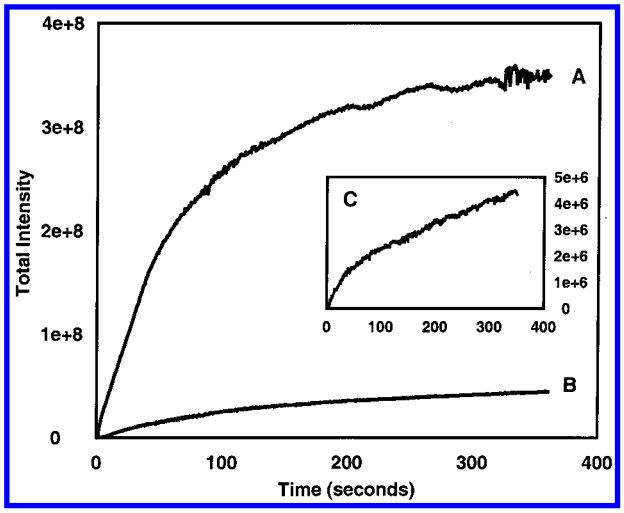

Figure 4. Total emission intensity vs time for three different excitation intensities at 514.5 nm: (A) 295 W/cm^2; (B) 77 W/cm^2; (C) 18 W/cm^2. All identical regions show an initial linearly increasing region that levels off to reach a steady-state nanocluster density (fluorescence intensity). Note that the data in (C) reach a final emission intensity that is nearly 2 orders of magnitude lower than that in (A), even though excitation is only a factor of 16 lower. Ratios of the initial slopes of (A), (B), and (C), yield a superlinear fluorescence intensity, I_F, dependence on excitation intensity, I_E, scaling as $I_F = I_E^{1.64\pm0.10}$.

creating Ag_n nanoclusters clearly dominates, favoring nanocluster creation at higher incident intensities and yielding a superlinear, but subquadratic, intensity dependence.

As oxygen atoms are produced in AgO photochemistry, environmental conditions will further affect Ag_n nanocluster dynamics and stability. Under moderate (10^{-5} Torr) vacuum, the activation rate dropped 11.7-fold relative to that in air at atmospheric pressure, whereas under both nitrogen and argon atmospheres, the final written fluorescence intensity increased 2-fold over ambient conditions. Writing fluorescent Ag_n nanoclusters in an O_2-enriched environment yields an activation rate slower than that in either Ar or N_2, but comparable to that in air. Because AgO is stable at room temperature, two processes must occur to generate stable Ag_n nanoclusters: removal of atomic oxygen and dissipation of energy. Including the optical excitation, AgO photodecomposition is exothermic, thereby requiring dissipation of the large amount of energy injected into the AgO system through light absorption. Evacuated environments provide insufficient collisional rates to dissipate excess energy, thereby favoring reactants in this exothermic photochemical reaction. As a result, photoactivation is significantly less efficient in a vacuum. Under even moderate vacuum conditions however, the lack of molecules present to undergo collisions hinders the system's ability to write data efficiently. As a result, though photoactivation still occurs in a vacuum, it is considerably slower than in ambient conditions. Although any gas will provide sufficient collisions to dissipate the excess energy and shift the equilibrium toward Ag_n nanoclusters, oxygen is a byproduct of the AgO photodecomposition and could promote nanocluster reoxidation to AgO. Due to these effects on the equilibrium between AgO and Ag, photoactivation is most efficient in nonevacuated, nonoxidizing environments. In fact, different nanocluster emission wavelengths are observed when excited in argon and nitrogen atmospheres, exhibiting significant emission even when excited with UV wavelengths. These presumably less stable nanoclusters are more easily oxidized back to nonfluorescent AgO but are stabilized in inert environments.

Through varied sample preparation and control of external conditions, we have elucidated the important chemical species involved in photoactivation of silver oxides. AgO films are readily photoactivated with UV excitation, preferably in inert atmospheres to produce highly fluorescent, surface-bound Ag_n nanoclusters. Because only nanoclusters containing 2−8 atoms are known to exhibit significant oscillator strengths at visible wavelengths,[15,16,17] and superlinear, but subquadratic intensity dependences of writing have been observed, we have obtained further evidence that the emissive species, as on cryogenic AgBr crystals, are small Ag_n nanoclusters. By understanding the molecular to bulk transition of this system with our single molecule and bulk methods, we can begin to harness its dynamics for exploring the role of these nanomaterials in optical data storage.

Acknowledgment. R.M.D. gratefully acknowledges support from the Alfred P. Sloan and Dreyfus Foundations.

References and Notes

(1) Moscowitz, M. *Rev. Mod. Phys.* **1985**, *57*, 783.
(2) Kneipp, K.; Wang, Y.; Kneipp, H.; Perelman, L. T.; Itzkan, I.; Dasari, R.; Feld, M. S. *Phys. Rev. Lett.* **1997**, *78*, 1667.
(3) Nie, S. M.; Emory, S. R. *Science* **1997**, *275*, 1102.
(4) Michaels, A. M.; Nirmal, M.; Brus, L. E. *J. Am. Chem. Soc.* **1999**, *121*, 9932.
(5) *Nanostructured Materials and Nanotechnology*; Nalwa, H. S., Ed.; Academic Press: New York, 2000.
(6) Timp, G. *Nanotechnology*; Springer-Verlag: New York, 1999.
(7) Ehrlich, S. H. *J. Imaging Sci. Technol.* **1993**, *37*, 73.
(8) Eachus, R. S.; Marchetti, A. P.; Muenter, A. A. *Annu. Rev. Phys. Chem.* **1999**, *50*, 117.
(9) Tominaga, J.; Haratani, S.; Uchiyama, K.; Takayama, S. *Jpn. J. Appl. Phys. Part 1 − Regul. Pap. Short Notes Rev. Pap.* **1992**, *31*, 2757.
(10) Peyser, L. A.; Vinson, A. E.; Bartko, A. P.; Dickson, R. M. *Science* **2001**, *291*, 103.
(11) Varkey, A. J.; Fort, A. F. *Sol. Energy Mater. Sol. Cells* **1993**, *29*, 253.
(12) Kocareva, T.; Grozdanov, I.; Pejova, B. *Mater. Lett.* **2001**, *47*, 319.
(13) Buchel, D.; Mihalcea, C.; Fukaya, T.; Atoda, N.; Tominaga, J.; Kikukawa, T.; Fuji, H. *Appl. Phys. Lett.* **2001**, *79*, 620.
(14) Xiong, Y.; Wu, H.; Guo, Y.; Sun, Y.; Yang, D.; Da, D. *Thin Solid Films* **2000**, *375*, 300.
(15) Rabin, I.; Schulze, W.; Ertl, G. *J. Chem. Phys.* **1998**, *108*, 5137.
(16) Harbich, W.; Fedrigo, S.; Meyer, F.; Lindsay, D. M.; Lignieres, J.; Rivoal, J. C.; Kreisle, D. *J. Chem. Phys.* **1990**, *93*, 8535.
(17) Bonacić-Koutecky, V.; Veyret, V.; Mitrić, R. *J. Chem. Phys.* **2001**, *115*, 10450.
(18) Weis, P.; Bierweiler, T.; Gilb, S.; Kappes, M. M. *Chem. Phys. Lett.* **2002**, *355*, 355.
(19) Bartko, A. P.; Dickson, R. M. *J. Phys. Chem. B* **1999**, *103*, 11237.
(20) Bartko, A. P.; Dickson, R. M. *J. Phys. Chem. B* **1999**, *103*, 3053.
(21) Ferrari, A. M.; Xiao, C.; Neyman, K. M.; Pacchioni, G.; Rosch, N. *Phys. Chem. Chem. Phys.* **1999**, *1*, 4655.
(22) Oku, Y.; Kawasaki, M. *J. Phys. Chem. B* **1998**, *102*, 9061.
(23) Geva, E.; Skinner, J. L. *Chem. Phys. Lett.* **1998**, *287*, 125.
(24) Lu, H. P.; Xie, X. S. *Nature* **1997**, *385*, 143.
(25) Empedocles, S. A.; Bawendi, M. G. *J. Phys. Chem. B* **1999**, *103*, 1826.
(26) Skinner, J. L.; Moerner, W. E. *J. Phys. Chem.* **1996**, *100*, 13251.
(27) Peyser, L. A.; Lee, T.-H.; Dickson, R. M. *Harnessing Single Particle Dynamics in Silver Nanomaterials*; SPIE, International Society of Optical Engineers: San Jose, CA, 2002.